Optical frequency-to-time mapping using a phase-modulated frequency-shifting loop

Hongzhi Yang, Marc Brunel, Marc Vallet, Haiyang Zhang, Changming Zhao

Optical frequency-to-time mapping using a phase-modulated frequency-shifting loop

HONGZHI YANG,[1,2,*] MARC BRUNEL,[3] MARC VALLET,[3] HAIYANG ZHANG,[1] AND CHANGMING ZHAO[1]

[1]School of Optics and Photonics, Beijing Institute of Technology, Beijing, China
[2]Qian Xuesen Laboratory of Space Technology, NO. 104 Youyi Road, Haidian district, Beijing, China
[3]Univ Rennes, CNRS, Institut FOTON – UMR 6082, 35000 Rennes, France
*Corresponding author: yanghongzhi@qxslab.cn

Received XX Month XXXX; revised XX Month, XXXX; accepted XX Month XXXX; posted XX Month XXXX (Doc. ID XXXXX); published XX Month XXXX

Real-time spectral analysis is demonstrated experimentally with a frequency-shifting loop that includes an electro-optic phase modulator. When a single-frequency laser seeds the loop, pulse doublets are emitted if the integer Talbot condition is satisfied. With a polychromatic seed, frequency-to-time mapping is demonstrated, namely the temporal output of the loop maps the spectral power of the seed, with a resolution of 400 kHz. Due to the phase modulation function, the mapping is shown to be nonlinear. All our results are in agreement with the theoretical predictions of [H. Yang et al., J. Opt. Soc. Am. B 37, 3162 (2020)]. Extension to integrated systems for applications is discussed. © 2021 Optical Society of America

http://dx.doi.org/10.1364/OL.99.099999

In recent years, significant progresses have been made in the use of photonic methods to achieve RF-waveform generation [1], processing [2-4], or transmission [5]. Among these methods, optical real-time Fourier transformation (RTFT) has received special attention because of its extraordinary processing speed, which is far beyond conventional digital signal processing methods [6].

Optical real-time Fourier transformation mainly relies on the ability to map the power spectral density of the input optical signal into a time-domain envelope, a process called frequency-to-time mapping (FTM). The idea was originally implemented using optical fibers or gratings with a large dispersion, which is often referred to as the dispersion method [6]. The fundamental problem of the dispersion method is that high spectral resolution requires a very large dispersion, which is accompanied by high optical losses. In order to overcome this drawback, an optical amplifier was inserted into the RTFT system [7]. Nonetheless, the frequency resolution of the dispersion method is still in the vicinity of tens of GHz. Some new methods have been investigated to further improve the frequency resolution, such as time-domain stretching techniques based on time lenses, discrete dispersion method, and frequency shifting loop (FSL). In the first case, the RF signal to be measured is converted into a time delay through a dispersion device, and the signal is then stretched by a time-lens to improve the frequency resolution [8-9]. In the discrete dispersion case, the dispersion device is specially designed, whereby the intensity response is set on and off periodically, with the phase frequency response being continuous and proportional to the square of the frequency [10]. Besides, frequency-shifting loops have shown an extraordinary performance in optical real-time Fourier transformation, with a frequency resolution reaching several kHz [11].

Frequency-shifting loops usually include an acousto-optic frequency shifter (AOFS) which shifts the optical frequency of the seed at each round-trip. While it features high frequency conversion efficiency in the sub-100 MHz range, the AOFS has limited efficiency in the GHz range. Besides, a FSL containing a single sideband electro-optic phase modulator (EOPM) was investigated to generate GHz repetition rates in the Talbot configuration [12], and electro-optic amplitude modulator leads to a specific pulse-doublet regime [13]. Recently, the ability of the phase-modulated frequency-shifting loop to perform optical real-time Fourier transformation was theoretically discussed in [14]. This theoretical model predicts that FTM can be observed in the EOPM-based FSL, with different features from the AOFS case. It is hence the aim of this paper to investigate experimentally such an EOPM-based FSL. It is worthwhile to note that EOPM could offer much higher bandwidth and are inherently integrated devices. Hence, by designing a micro-ring which includes an EOPM and a fiber-coupled semiconductor optical amplifier (SOA) to significantly shorten the loop length (or increase fundamental frequency), the proposed optical FTM would become fully integrable in a high-bandwidth microsystem.

Our set-up is based on a phase-modulated FSL as depicted in Fig.1. The seed is a tunable single-frequency laser (SFL), which delivers 0.3 mW at around 1550 nm in the C band. It is modulated

by an electro-optic modulator (EOPM1), that is driven by a waveform generator (RF-IN). The FSL contains another electro-optic phase modulator (EOPM2) that induces the dual-sideband frequency shift $\pm f_m$, an optical amplifier (EDFA) to compensate for the losses, and a tunable bandpass filter (TBPF) providing spectral filtering to circumvent spurious active mode-locking induced by the spontaneous emission in the EDFA. The polarization controller (PC) and a polarizer (not shown) are used to stabilize the polarization state of the circulating seed laser. The loop delay time we measured to be $\tau = 0.112$ μs, corresponding to a fundamental frequency $f_c = 8.943$ MHz. The detection set-up consists in a 40 GHz bandwidth photodiode (PD) and a high-resolution optical spectrum analyzer (OSA). In the time domain, the signal is monitored by an 11 GHz-bandwidth, 40 Gs/s sampling-rate, oscilloscope.

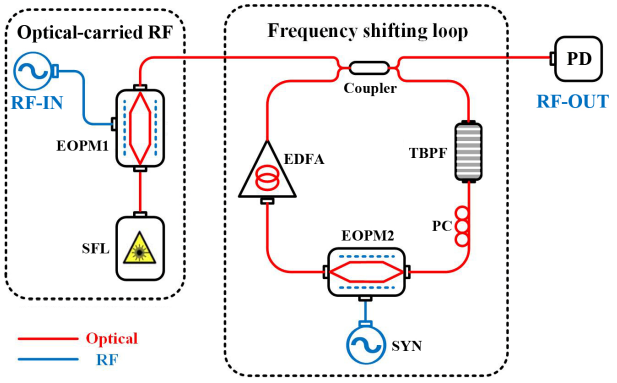

Fig. 1. Experimental set-up. See text for details.

Before describing our exeprimental results, let us recall briefly the predictions from the model of Ref. [14]. When the loop is fed by an optical wave at angular frequency ω_0 and power P_0, the loop output power is calculated to be $P_{out}(t) = \left|t_{11} + \frac{t_{21}t_{12}}{t_{22}} L(t)\right|^2 P_0$, where $[t_{ij}]$ is the transmission matrix of the coupler. The loop function $L(t)$ contains the sum of all, time-delayed, up- and down-shifted frequency components circulating inside the loop. In the integer Talbot condition $f_m = pf_c$, it can be simply written as

$$L(t) = \frac{t_{22}\gamma e^{j\theta(t)}}{1 - t_{22}\gamma e^{j\theta(t)}}, \qquad (1)$$

γ being a constant real parameter that includes loss and gain factors inside the loop, and

$$\theta(t) = \delta \sin(2\pi f_m t) + \omega_0 \tau, \qquad (2)$$

where δ is the modulation depth of the phase modulator. From Eqs. (1)-(2), one finds that the output power is a function peaked in $\theta(t) = 2k\pi$ ($k \in \mathbb{Z}$), with a repetition rate f_m. This is the basis of the FTM process : one optical frequency at the input yields a pulse at the output. However, due to the sine function in Eq. (2), one single optical frequency will induce a doublet of pulses per period. Of course this result depends on the value of δ, but the simplest scenario is obtained when $\delta = \pi$ [14], a condition that we will maintain in the present experimental study. Then a narrow bandwidth spectrum will result in a peculiar frequency-to-time mapping, where both the input spectrum *and its mirror image* will be mapped over one period. Besides, due to the $(\omega_0\tau)$ term, two optical frequencies separated by multiples of the fundamental frequency $f_m = 1/\tau$ will produce identical time traces. Hence, to ensure that the FTM process is achieved unambiguously, the frequency bandwidth of the seed laser should be kept smaller than f_c. Another finding of the simulations is that the ratio of the pulse width to the pulse period is always the same regardless of the value of p. Finally, it is important to note that real-time Fourier transform can be obtained only provided that the solutions of Eq. (2) stay in the linear region of the sine function (ideally $\omega_0\tau = 2k'\pi, k' \in \mathbb{Z}$). Conversely, when the solutions are out of the linear region, this EO-PM configuration performs nonlinear FTM.

Let us now describe the experimental results, where we look for evidences of (i) pulse doublets in the integer Talbot condition, (ii) FTM process with the peculiar mirror effect, and (iii) ambiguity characterization. We first check the loop reponse with an un-modulated, single-frequency source seeding the loop in an integer Talbot condition $f_m = pf_c$. It is found that the output time traces are pulse doublets with a repetition rate f_m, in agreement with the theoretical results. The model predicts that the interval between the doublet pulses depends on the input optical frequency and on the modulating depth of the phase modulator. Here the RF power provided by the synthesizer is set to 25 dBm, an experimental value that is found to satisfy the requirement of one-to-one mapping, namely the modulating depth is equal to π.

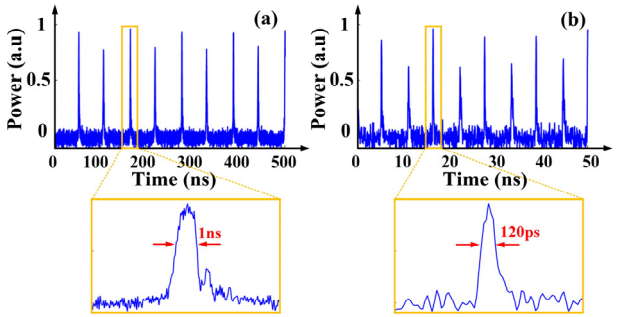

Fig. 2 Experimental pulse doublets. Response of PM-FSL to the single-frequency laser in integer Talbot conditions (a) $p = 1$ and (b) p=10.

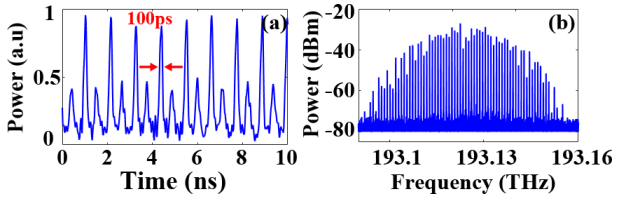

Fig. 3. Experimental pulse doublets. Response of PM-FSL to the single-frequency laser when p=100: (a) time trace; (b) optical spectrum.

Fig. 2 reproduces the output traces when $p = 1$ and $p = 10$, respectively. The response of the PM-FSL to the single-frequency seed laser is a periodic train of pulse-doublets with a pulse width of about 1 ns, and 120 ps, respectively. When we further increase the RF frequency shift to $f_m = 100f_c$, the pulse wide is measured to be 100 ps as shown in Fig.3(a). The pulse-width measurement is limited by the 11 GHz-bandwidth of the oscilloscope. In order to precisely evaluate the optical spectrum of the output waveform,

the signal is measured by using a 5 MHz-resolution OSA. The output optical spectrum confirms the limitation of the detection setup, because, as shown in Fig. 3(b), the total width of the optical spectrum is over 70 GHz at –20 dB (which corresponds to ps-scale pulses). It is worth to note that the bandwidth of the TBPF is 0.3 nm corresponding to about 40 GHz FWHM.

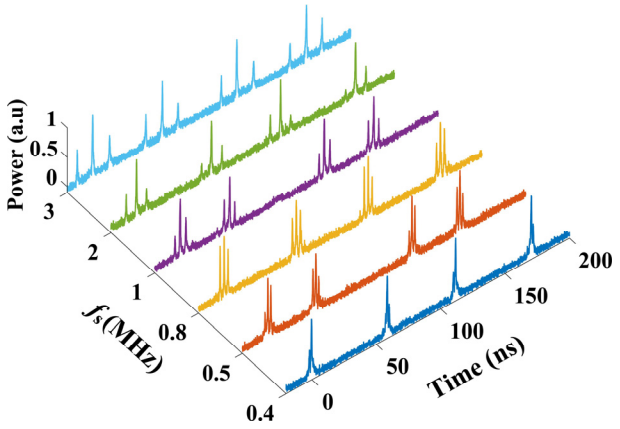

Fig. 4. Experimental waveforms when the RF power applied to the EOPM1 is 5 dBm; The SFL is phase-modulated by a RF at different frequencies 400kHz, 500kHz, 800kHz, 1MHz, 2MHz and 3MHz.

Secondly, we analyze the FTM property of this loop. The SFL is now modulated by EOPM1 at frequency f_s in order to generate a multi-tone input. The RF f_m applied to the EOPM2 (inside the loop) is kept at integer multiple of the fundamental loop frequency to meet the Talbot condition $f_m = pf_c$. We choose $f_m = 8.9$ MHz ($p = 1$). When the RF power applied to EOPM1 is 5 dBm, experimental results are shown in Fig. 4. Compared with the results in Fig. 2, three pairs of pulse-doublets are observed in one modulation period. Interestingly, due to the sinusoidal phase in the loop function, the FTM process presents a mirror effect (see the unbalanced sidebands amplitudes on one side or the other of the main pulse). In addition, we verify that as the RF applied to the EOPM1 decreases from $f_s = 3$ MHz to $f_s = 400$ kHz, the interval between the output pulses gradually decreases. These experimental results prove that the spectrum of the laser at the input of FSL is efficiently mapped to the intensity time signal at the output.

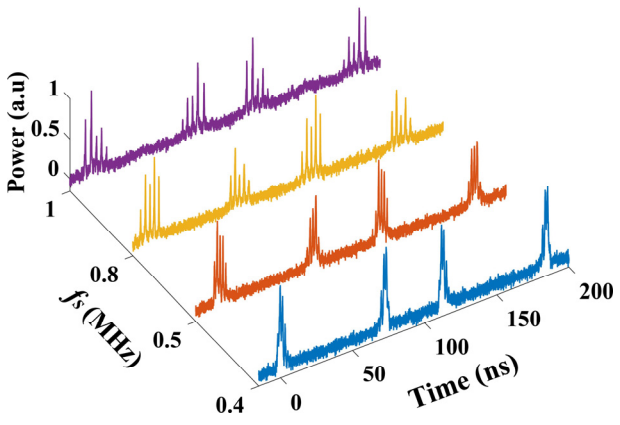

Fig. 5. Experimental waveforms when the RF power applied to the EOPM1 is 10 dBm; The SFL is phase-modulated by a RF at different frequencies 400kHz, 500kHz, 800kHz and1MHz.

To further observe the phenomenon of the optical real-time Fourier transformation, the RF power applied to EOPM1 increases to 10 dBm, which aims at generating more sidebands. We keep $f_m = f_c$. Again, the output traces with different modulating frequencies (f_s) are measured, as shown in Fig. 5. Compared with the experimental results in Fig. 4, five pairs of pulse-doublets are observed in one period τ_m. As expected, the pulse-doublets present the mirror effect in the FTM, and the interval between the different side-pulses decreases as the modulating frequency f_s decrease from 1 MHz to 400 kHz. From these observations we evaluate the resolution to be 400 kHz.

In line with the theoretical model, the unambiguity frequency of the proposed RTFT is limited by the fundamental frequency of the FSL. To experimentally verify this property without changing the input optical frequency ω_0, the RF f_s applied to the EOPM1 is set successively to 9.9 MHz ($f_c + 1$ MHz) and 18.8 MHz ($2f_c + 1$ MHz), respectively, while the RF power applied to EOPM1 is kept at 5 dBm. We keep $f_m = f_c$. The output time traces are shown in Fig. 6. The envelopes of the output signal are the same even though values of f_s are different, which proves that the fundamental frequency of the FSL determines the unambiguity frequency.

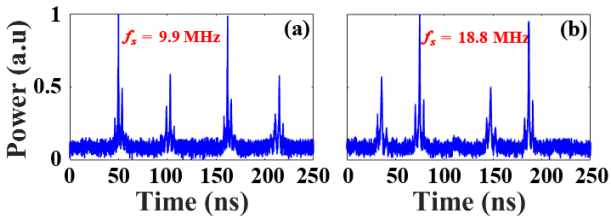

Fig. 6. Ambiguity in the FTM process: (a) $f_s = 9.9$ MHz ;(b) $f_s = 18.8$ MHz

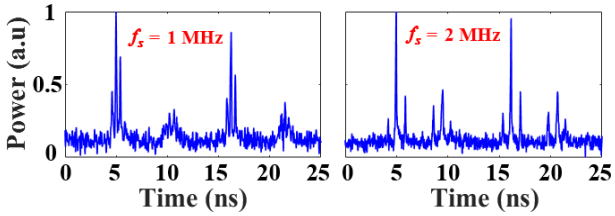

Fig. 7. FTM process when $f_m = 10f_c$. (a) $f_s = 1$ MHz ; (b) $f_s = 2$ MHz.

We also check that the resolution is independent on p (integer Talbot condition). We increase the frequency shift from $f_m = f_c$ (Fig. 6) to $f_m = 10\,f_c$ and plot the output traces, as shown in Fig. 7. The RF f_s generating the optical sidebands of the seed laser is adjusted successively to 1 MHz and 2 MHz, respectively. It is obvious that the envelopes of the output traces are the same (see Figs. 6(a) and 7(a)) Compared with $f_m = f_c$, the repetition rate scales as 10, but the pulse duration also scales as 1/10. The experiment results support the theoretical prediction of the Talbot effect and also indicate that the frequency resolution in the RTFT process keeps the same for all Talbot orders p. One can conclude that the optical frequency

resolution is simply determined by the circulating time of the seed laser inside the loop.

Finally, to characterize the sinusoidal frequency-to-time mapping property, the relationship between the peak positions in time domain and the input optical frequencies is investigated, as shown in Fig. 8. The frequency shift f_m inside the loop is equal to the fundamental loop frequency f_c. The input optical spectrum is an optical comb with 5 teeth, and the frequency interval is 1MHz. Different from the linear frequency-to-time mapping property in the acousto-optic frequency shifter based FSL, we verify that the peak positions in the time domain is sinusoidally dependent on the input optical frequency. The comb of evenly shifted side-bands is converted to a sequence of nonlinearly spaced pulses.

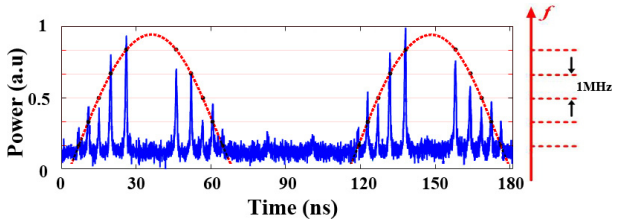

Fig. 8. Illustration of nonlinear FTM. Sinusoidal modulation (red dotted curve) and output waveform (blue line curve). 1 MHz frequency steps are converted to nonlinear inter-pulse intervals.

In conclusion, we have demonstrated the pulse-doublets regime by using a phase-modulated FSL seeded by a single-frequency laser. The interval between the pulse-doublet is dependent on the optical frequency of the seed laser and the fundamental frequency of the loop. In principle, the interval could be used to evaluate the instantaneous frequency drift of the seed laser assuming that the modulating depth is known and the loop is well stabilized [Eq. (2)]. We also evidence the relationship between the optical spectrum at the input and the output time traces, namely the realization of the RTFT. The experimental resolution is shown to be 400 kHz (without averaging) determined by the number of comb lines inside the loop. One could improve the resolution by increasing the net gain coefficient and reducing the ASE noise simultaneously [15]. Thus, choosing an optical amplifier with much lower noise factor (NF) will be a direct and effective method. When kHz resolutions are sought, f_m should be minimized while keeping the Talbot condition, that is $f_m = f_c$. In the AOFS-based FSL, two AOFS with opposite orientations are required because of the limited bandwidth. Here, the broad bandwidth of the EOPM, from kHz to dozens of GHz, simplifies the FSL system.

When looking for large processing bandwidths, downsizing the loop could be a solution. Indeed, the bandwidth of the signal to be processed is limited by the fundamental loop frequency, meaning that an unknown input optical spectrum can be inferred without ambiguity if its spectral bandwidth is smaller than f_c. Benefiting from the rapid development of integrated photonics, micro-rings seeded by fiber-coupled semiconductor lasers have been widely used in micro-resonator optical frequency comb generation [16-17]. Silicon photonic integrated circuits for telecommunication and data centers have been well studied [18]. An integrated FSF laser based on a doped lithium niobate waveguide has been previously demonstrated, and a value of f_c larger than 700 MHz was reported [19]. Thus, designing a micro-ring that includes the state-of-art monolithic semiconductor laser, semiconductor amplifier and integrated EOPM would permit to significantly shorten the loop length leading to a fully integrable high-bandwidth real-time spectral analyzer microsystem. The proof-of-concept demonstrated here could also find applications like pulse compressed lidar [20], arbitrary waveform generation and velocimetry [21]. For example, in velocity measurements, direct detection of targets moving at speeds as low as a few centimeters per second is possible by real-time measurement of the Doppler frequency shift.

Funding. Région Bretagne, FEDER (EU), and Rennes Metropole (CPER SOPHIE-Photonique). H. Yang was the recipient of a Chinese Scholarship Council (CSC) grant.

Disclosures. The authors declare no conflicts of interest.

References

1. P. S. Devgan, *Applications of Modern RF Photonics* (Artech House, 2018).
2. J. Capmany, J. Mora, I. Gasulla, J. Sancho, J. Lloret, and S. Sales, J. Lightwave Technol. **31**, 571 (2013).
3. Z. Jiang, C. Huang, D. Leaird, and A. M. Weiner, Nature Photon. **1**, 463 (2007).
4. P. J. Delfyett, S. Gee, M. Choi, H. Izadpanah, W. Lee, S. Ozharar, F. Quinlan, and T. Yilmaz, J. Lightwave Technol. **24**, 2701 (2006).
5. J. Yu, J. Hu, D. Qian, Z. Jia, G. Chang, and T. Wang, in *Conference on Optical Fiber Communication/National Fiber Optic Engineers Conference* (IEEE, 2008).
6. M. A. Muriel, J. Azaña, and A. Carballar, Opt. Lett. **24**, 1 (1999).
7. D. R. Solli, J. Chou, and B. Jalali, Nature Photon. **2**, 48 (2008).
8. Y. Duan, L. Chen, H. Zhou, X. Zhou, C. Zhang, and X. Zhang, Opt. Express **25**, 7520 (2017).
9. Y. Duan, L. Chen, H. Zhou, X. Zhou, C. Zhang, and X. Zhang, Opt. Express **26**, 20735 (2018).
10. Y. Dai, J. Li, Z. Zhang, F. Yin, W. Li, and K. Xu, Opt. Express **25**, 16660 (2017).
11. H. Guillet de Chatellus, L. R. Cortés, and J. Azaña, Optica **3**, 1 (2016).
12. L. Wang and S. LaRochelle, in *Conference on Lasers and Electro-Optics*, OSA Technical Digest (OSA, 2017), paper JW2A.66.
13. H. Yang, M. Vallet, H. Zhang, C. Zhao, and M. Brunel, Opt. Express **27**, 18766 (2019).
14. H. Yang, M. Brunel, M. Vallet, H. Zhang, and C. Zhao, J. Opt. Soc. Am. B, **37**, 3162-3169 (2020).
15. N. Kanagaraj, L. Djevarhidjian, V. Duran, C. Schnebelin, and H. Guillet de Chatellus, Opt. Express **27**, 14842 (2019)
16. L. Chang, W. Xie, H. Shu, Q. Yang, B. Shen, A. Boes, J. D. Peters, W. Jin, C. Xiang, S. Liu, G. Moille, S. Yu, X. Wang, K. Srinivasan, S. B. Papp, K. Vahala and J. E. Bowers, Nat. Commun. **11**, 1331 (2020).
17. Z. L. Newman, V. Maurice, T. Drake, J. R. Stone, T. C. Briles, D. T. Spencer, C. Fredrick, Q. Li, D. Westly, B. R. Ilic, B. Shen, M. Suh, K. Youl Yang, C. Johnson, D. M. S. Johnson, L. Hollberg, K. J. Vahala, K. Srinivasan, S. A. Diddams, J. Kitching, S. B. Papp, and M. T. Hummon, Optica **6**, 680 (2019)
18. Y. Bie, G. Grosso, M. Heuck, M. M. Furchi, Y. Cao, J. Zheng, D. Bunandar, E. Navarro-Moratalla, L. Zhou, D. K. Efetov, T. Taniguchi, K. Watanabe, J. Kong, D. Englund and P. Jarillo-Herrero, Nature Nanotech **12**, 1124 (2017).
19. S. Reza, R. Ricken, V. Quiring, and W. Sohler, in European Conference on Lasers and Electro-Optics, Conference Digest (Optical Society of America, 2007), paper CJ3-5 (2007).
20. J. Clement, C. Schnébelin, H. Guillet de Chatellus, and C. R. Fernández-Pousa, Opt. Express **27**, 12000 (2019).
21. H. Yang, M. Brunel, H. Zhang, M. Vallet, C. Zhao, and S. Yang, IEEE Photonics J. **9**, 7106609 (2017).

Fifth page list of full References

1. P. S. Devgan, *Applications of Modern RF Photonics* (Artech House, 2018).
2. J. Capmany, J. Mora, I. Gasulla, J. Sancho, J. Lloret, and S. Sales, "Microwave photonic signal processing," J. Lightwave Technol. **31**, 571 (2013).
3. Z. Jiang, C. Huang, D. Leaird, and A. M. Weiner, "Optical arbitrary waveform processing of more than 100 spectral comb lines," Nature Photon. **1**, 463 (2007).
4. P. J. Delfyett, S. Gee, M. Choi, H. Izadpanah, W. Lee, S. Ozharar, F. Quinlan, and T. Yilmaz, "Optical Frequency Combs From Semiconductor Lasers and Applications in Ultrawideband Signal Processing and Communications," J. Lightwave Technol. **24**, 2701 (2006).
5. J. Yu, J. Hu, D. Qian, Z. Jia, G. Chang, and T. Wang, " Transmission of microwave-photonics generated 16Gbit/s super broadband OFDM signals in radio-over-fiber system," in *Conference on Optical Fiber Communication/National Fiber Optic Engineers Conference* (IEEE, 2008).
6. M. A. Muriel, J. Azaña, and A. Carballar, "Real-time Fourier transformer based on fiber gratings," Opt. Lett. **24**, 1 (1999).
7. D. R. Solli, J. Chou, and B. Jalali, "Amplified wavelength–time transformation for real-time spectroscopy," Nature Photon. **2**, 48 (2008).
8. Y. Duan, L. Chen, H. Zhou, X. Zhou, C. Zhang, and X. Zhang, "Ultrafast electrical spectrum analyzer based on all-optical Fourier transform and temporal magnification," Opt. Express **25**, 7520 (2017).
9. Y. Duan, L. Chen, H. Zhou, X. Zhou, C. Zhang, and X. Zhang, "Temporal radio-frequency spectrum analyzer, based on asynchronous optical sampling assisted temporal convolution," Opt. Express **26**, 20735 (2018).
10. Y. Dai, J. Li, Z. Zhang, F. Yin, W. Li, and K. Xu, "Real-time frequency-to-time mapping based on spectrally-discrete chromatic dispersion," Opt. Express **25**, 16660 (2017).
11. H. Guillet de Chatellus, L. R. Cortés, and J. Azaña, "Optical real-time Fourier transformation with kilohertz resolutions," Optica **3**, 1 (2016).
12. L. Wang and S. LaRochelle, "Talbot Laser with Tunable GHz Repetition Rate using an Electro-Optic Frequency Shifter," in *Conference on Lasers and Electro-Optics*, OSA Technical Digest (OSA, 2017), paper JW2A.66.
13. H. Yang, M. Vallet, H. Zhang, C. Zhao, and M. Brunel, "Pulse doublets generated by a frequency-shifting loop containing an electro-optic amplitude modulator," Opt. Express **27**, 18766 (2019).
14. H. Yang, M. Brunel, M. Vallet, H. Zhang, and C. Zhao, "Analysis of frequency-shifting loops in integer and fractional Talbot conditions: electro-optic vs acousto-optic modulation," J. Opt. Soc. Am. B, **37**, 3162-3169 (2020).
15. N. Kanagaraj, L. Djevarhidjian, V. Duran, C. Schnebelin, and H. Guillet de Chatellus, "Optimization of acousto-optic optical frequency combs," Opt. Express **27**, 14842 (2019)
16. L. Chang, W. Xie, H. Shu, Q. Yang, B. Shen, A. Boes, J. D. Peters, W. Jin, C. Xiang, S. Liu, G. Moille, S. Yu, X. Wang, K. Srinivasan, S. B. Papp, K. Vahala and J. E. Bowers, "Ultra-efficient frequency comb generation in AlGaAs-on-insulator microresonators," Nat. Commun. **11**, 1331 (2020).
17. Z. L. Newman, V. Maurice, T. Drake, J. R. Stone, T. C. Briles, D. T. Spencer, C. Fredrick, Q. Li, D. Westly, B. R. Ilic, B. Shen, M. Suh, K. Youl Yang, C. Johnson, D. M. S. Johnson, L. Hollberg, K. J. Vahala, K. Srinivasan, S. A. Diddams, J. Kitching, S. B. Papp, and M. T. Hummon, "Architecture for the photonic integration of an optical atomic clock," Optica **6**, 680 (2019)
18. Y. Bie, G. Grosso, M. Heuck, M. M. Furchi, Y. Cao, J. Zheng, D. Bunandar, E. Navarro-Moratalla, L. Zhou, D. K. Efetov, T. Taniguchi, K. Watanabe, J. Kong, D. Englund and P. Jarillo-Herrero, "A MoTe2-based light-emitting diode and photodetector for silicon photonic integrated circuits," Nature Nanotech **12**, 1124 (2017).
19. S. Reza, R. Ricken, V. Quiring, and W. Sohler, "High resolution optical frequency domain ranging with an integrated frequency shifted feedback (FSF) laser," in European Conference on Lasers and Electro-Optics, Conference Digest (Optical Society of America, 2007), paper CJ3-5 (2007).
20. J. Clement, C. Schnébelin, H. Guillet de Chatellus, and C. R. Fernández-Pousa, "Laser ranging using coherent pulse compression with frequency shifting loops," Opt. Express **27**, 12000 (2019).
21. H. Yang, M. Brunel, H. Zhang, M. Vallet, C. Zhao, and S. Yang, "RF Up-Conversion and Waveform Generation Using a Frequency-Shifting Amplifying Fiber Loop, Application to Doppler Velocimetry," IEEE Photonics J. **9**, 7106609 (2017).